J Mater Sci (2010) 45:701–705
DOI 10.1007/s10853-009-3987-5

Wear characteristics of a new type austenitic stainless steel

**Jianjian Ye · Zhiwei Lai · Yuhua Wen ·
Ning Li**

Received: 1 June 2009 / Accepted: 13 October 2009 / Published online: 4 November 2009

Abstract In order to solve the problem of the poor wear resistance in conventional austenitic stainless steels, a new type austenitic stainless steel was designed based on Fe–Mn–Si–Cr–Ni shape memory alloys in this article. Studies on its wear resistance and wear mechanism have been carried out by comparison with that of AISI 321 stainless steel using friction wear tests, X-ray diffraction, scanning electron microscope. Results showed that the wear resistance of Fe–14Mn–5.5Si–12Cr–5Ni–0.10C alloy was better than that of AISI 321 stainless steel both in dry and oily friction conditions owing to the occurrence of the stress-induced $\gamma \rightarrow \varepsilon$ martensitic phase transformation during friction process. This article also compared the corrosion performance of the two stainless steels by testing the corrosion rate. Results showed that the corrosion rate of Fe–14Mn–5.5Si–12Cr–5Ni–0.10C alloy was notably lower in NaOH solution and higher in NaCl solution than that of AISI 321 stainless steel.

Introduction

The Cr–Ni austenitic stainless steels are widely used for structural applications in kinds of chemical processing areas for their excellent corrosion resistance characteristic, mechanical properties, processing performance, solderability, and so on. However, their low hardness and poor wear resistance limit some of their applications. To solve this problem, kinds of surface modification, such as carburizing [1], nitriding [2, 3], and surface laser cladding [4–6], were adopted. However, the surface modification, on the one hand, damaged the corrosion resistance to some degree [7, 8]. On the other hand, the hard coating is prone to depart from the substrate under sliding friction or impact and it is difficult to prepare a large size component [9].

Studies showed that Fe–Mn–Si–Cr–Ni shape memory alloys enjoyed good corrosion and intergranular corrosion resistance in some corrosive environment besides their unique shape memory effect [10, 11]. Furthermore, the shape memory effect in Fe–Mn–Si–Cr–Ni alloys resulted from the stress-induced $\gamma \rightarrow \varepsilon$ martensitic phase transformation and its reverse transformation [12–15]. Theoretically, the occurrence of the stress-induced $\gamma \rightarrow \varepsilon$ martensitic transformation can absorb friction energy and thus reduce the plastic deformation. As a result, the formation and development of crackle can be blocked. At the same time, the close-packed hexagonal ε martensite, product of the stress-induced $\gamma \rightarrow \varepsilon$ martensitic transformation, which is induced by the wear process, has a higher hardness and lower adhesive coefficient than the face-centered cubic γ austenite. Accordingly, Fe–Mn–Si–Cr–Ni shape memory alloys are expected to possess a good wear resistance. In fact, Lin et al.'s [16] studies showed that Fe–17Mn–5Si–10Cr–4Ni alloy exhibited better wear resistance performance in oily friction, but poorer in dry friction than AISI 321 stainless steels. They attributed the poor wear resistance in dry friction to no occurrence of the stress-induced $\gamma \rightarrow \varepsilon$ martensitic transformation.

As is well known, the carbon solution in austenite, on the one hand, can strengthen austenite and improve the wear resistance of Fe–Mn–Si–Cr–Ni shape memory alloys. On the other hand, the allowance of higher carbon content will remarkably decrease the production cost of Fe–Mn–Si–Cr–Ni-based shape memory alloys because cheap raw materials, such as scrap steel, can be used instead of

J. Ye · Z. Lai · Y. Wen (✉) · N. Li
College of Manufacturing Science and Engineering, Sichuan University, Chengdu 610065, People's Republic of China
e-mail: wenyh-mse@126.com

expensive pure metal. Therefore, it is of significance to investigate the effect of carbon addition on the wear resistance of Fe–Mn–Si–Cr–Ni-based shape memory alloys.

In this article, a new Fe–14Mn–5.5Si–12Cr–5Ni–0.10C alloy was designed. The chromium content in this new alloy was higher than that of the conventional Fe–Mn–Si–Cr–Ni-based shape memory alloys with the purpose of further improving its corrosion resistance. The carbon element was added to further improve the wear resistance and reduce the cost of raw materials. Results showed that Fe–14Mn–5.5Si–12Cr–5Ni–0.10C alloy exhibited better wear resistance than that of AISI 321 stainless steel under both oily and dry friction conditions. Meanwhile, compared with AISI 321 stainless steel, Fe–14Mn–5.5Si–12Cr–5Ni–0.1C alloy exhibited better in NaOH solution, while poorer in NaCl solution during the corrosion test.

Experimental materials and methods

The Fe–Mn–Si–Cr–Ni–C alloy was prepared by induction melting under an argon atmosphere, using high-purity iron, manganese, silicon, chromium, nickel, and graphite. After homogenization at 1373 K for 15 h, the ingot was forged into the bars 15 mm in diameter at 1373 K. Then, the bars were solution treated at 1373 K for 40 min. The chemical composition of the experimental alloy was listed in Table 1. The chemical composition of AISI 321 stainless steel, as a comparison alloy, was also listed in Table 1.

Cubical samples with 10 mm × 10 mm × 10 mm were cut from the solution-treated bars. The wear test was carried out on a M200 Wear Test Machine with pin-on-disk conduct sliding friction at a speed of 0.963 m/s for 60 min in dry and oily friction conditions, respectively. The friction coupled pair consisted of a cubical sample and a friction ring of GCr15 steel. The average hardness of GCr15 steel friction rings was 63HRC. An electronic balance Sartorius BS224S with the accuracy of 0.1 mg was used to measure the weight losses of the samples. Each presented value was the average value of three tested samples.

The corrosion test was carried out by immerging mechanically polished samples into a 3.5 wt% sodium chloride (NaCl) and a 3 mol/L sodium hydroxide (NaOH) solution at room temperatures (287–300 K), respectively. After immerging for days, the weight losses of the samples were determined using an electronic balance Sartorius BS224S with the accuracy of 0.1 mg. The corrosion resistance was evaluated by the corrosion rate (*V*), which was calculated using formula (1). Each presented value was the average value of three tested samples.

$$V\left(\mathrm{g/m^2/h}\right) = \frac{\Delta m}{At} \tag{1}$$

where Δm is the weight loss, A is the surface area of the sample, t is the time.

Phases in the surface of samples were identified using a X′ Pert Pro MPD X-ray diffraction (XRD) apparatus. The X-ray source was the Cu-K_α. The worn surface morphology of sample was analyzed using JSM-5910LV type scanning electron microscope (SEM).

Table 1 Chemical compositions of two alloys (wt%)

Alloys	Mn	Si	Cr	Ni	C	Ti	Fe
Fe–Mn–Si–Cr–Ni–C	13.95	5.67	11.54	5.36	0.11	–	Bal.
AISI 321	–	–	17.80	7.92	0.07	0.52	Bal.

Results

Figure 1 shows the weight loss of Fe–Mn–Si–Cr–Ni–C alloy and AISI 321 stainless steel under different loads in dry and oily friction conditions, respectively. The weight loss in two alloys both increased with increasing the load in two different conditions, but the weight loss in oily friction condition was lower than that in dry friction condition. Note that the weight loss of Fe–Mn–Si–Cr–Ni–C alloy was remarkably lower than that of AISI 321 stainless steel in dry and oily friction conditions, respectively.

Figure 2 shows the XRD patterns of the solution-treated Fe–Mn–Si–Cr–Ni–C alloy and after dry and oily friction conditions under 150 N, respectively. For the solution-treated Fe–Mn–Si–Cr–Ni–C alloy, the dominating phase was austenite. However, it is very clear that ε martensite was introduced after both dry and oily friction processes.

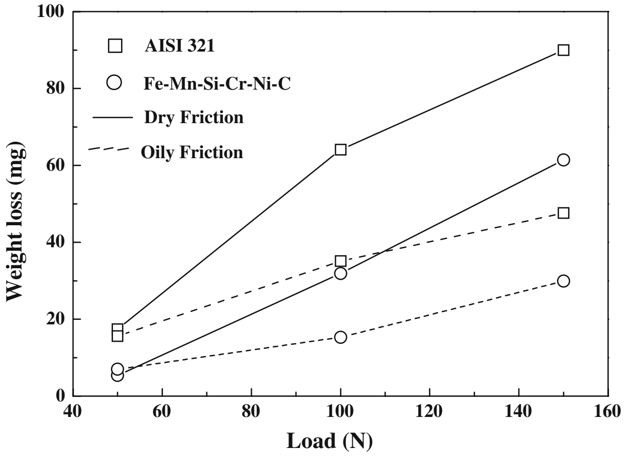

Fig. 1 The weight loss of Fe–Mn–Si–Cr–Ni–C alloy and AISI 321 stainless steel under the loads of 50, 100, and 150 N for 60 min in dry and oily friction conditions, respectively

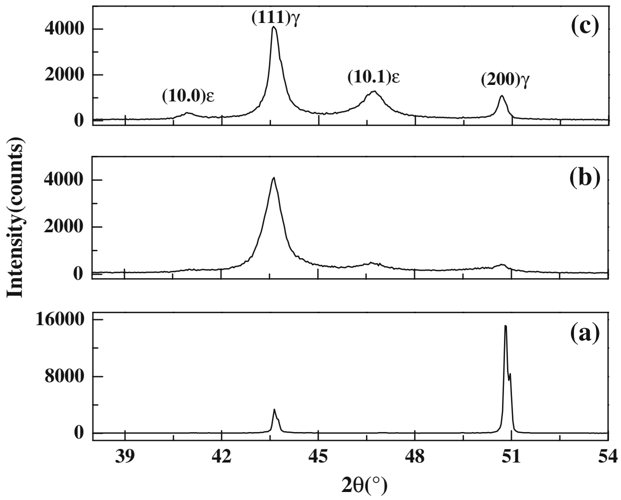

Fig. 2 XRD patterns for the surface of Fe–14Mn–5.5Si–12Cr–5Ni–0.10C alloy: **a** solution treated; **b** after dry friction under the load of 150 N; **c** after oily friction under the load of 150 N

Furthermore, more ε martensite was introduced after the oily friction process.

Figure 3 shows the worn surface morphology of AISI 321 stainless steel and Fe–Mn–Si–Cr–Ni–C alloy after oily and dry friction processes under the load of 150 N for 60 min, respectively. After dry friction, there existed serious tears on the surface of AISI 321 stainless steel, while only shallow furrows as well as mild tears on the surface of Fe–Mn–Si–Cr–Ni–C alloy. After oily friction, the worn surface of Fe–Mn–Si–Cr–Ni–C alloy was good and few tears and solders occurred, while there existed obvious tears and solders on the surface of AISI 321 stainless steel.

Table 2 Corrosion rate of two alloys

Alloys	R_{corr} (mg/m^2/h)	
	3.5 wt% NaCl	3 mol/L NaOH
Fe–14Mn–5.5Si–12Cr–5Ni–0.10C	0.9	0.2
AISI 321	0.5	0.7

Table 2 shows the corrosion rate of Fe–Mn–Si–Cr–Ni–C alloy and AISI 321 stainless alloy immerged in NaCl and NaOH solutions, respectively. The corrosion rate of Fe–Mn–Si–Cr–Ni–C alloy was remarkably lower in NaOH solution and higher in NaCl solution than that of AISI 321 stainless steel.

Discussion

The shape memory effect in Fe–Mn–Si–Cr–Ni alloys resulted from the stress-induced γ → ε martensitic transformation. In

Fig. 3 SEM micrographs of the worn surface of two alloys under the load of 150 N for 60 min: **a**, **c** oily friction; **b**, **d** dry friction

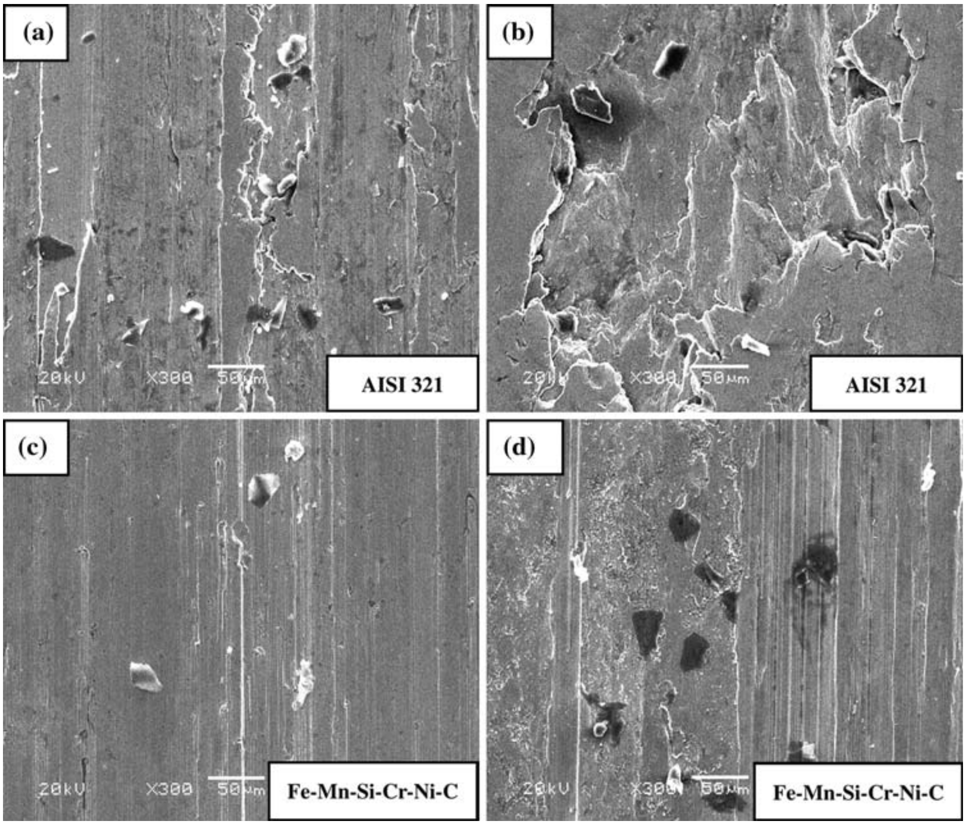

other words, the deformation takes place preferentially by stress-induced ε martensitic transformation, not by dislocations slip. Accordingly, stress-induced ε martensitic transformation would preferentially occur during friction at room temperature in Fe–14Mn–5.5Si–12Cr–5Ni–0.10C shape memory alloy. The results of XRD analysis confirmed that stress-induced ε martensitic transformation did occur in Fe–14Mn–5.5Si–12Cr–5Ni–0.10C shape memory alloy after both dry and oily friction processes. The occurrence of the stress-induced ε martensitic transformation, on the one hand, would absorb parts of friction energy and relax crack-tip stress, suppressing the formation of the crackles. On the other hand, the higher hardness and lower adhesive coefficient of the product ε martensite could block the occurrence of adhesive wear.

In oily friction, the lubricant could lay over the interface of the friction coupled pair, avoiding their direct contact and reducing wear to some degree. In addition, the lubricant could cool the friction coupled pair, favoring the occurrence of the stress-induced $\gamma \rightarrow \varepsilon$ martensitic transformation. Under dry friction condition, the high shear stress at contact occurred at the very start of wear test, thus the stress-induced $\gamma \rightarrow \varepsilon$ martensitic transformation would occur and ε martensite be induced. However, as the wear test went on, not only some stress-induced martensite would be gradually removed due to the high shear stress at contact, but also the temperature of the friction coupled pair rose because of the lack of oil cooling. As the result of the rise in temperature, the critical stress for stress-induced ε martensite was higher. Therefore, the occurrence of stress-induced ε martensitic transformation was suppressed and the amount of fresh stress-induced ε martensite decreased. When the temperature of the friction coupled pair was increased up to above the starting temperature of ε martensite to austenite transformation, the ε martensite which was not removed during the friction process would revert to austenite. This is the reason that more ε martensite was introduced in oily friction than in dry friction.

The austenite of AISI 321 stainless steel is very stable and thus no phase transformation occurs during wear at room temperature. Furthermore, the lower hardness and higher adhesive coefficient of austenite would promote the occurrence of adhesive wear especially in dry friction. As a result, there existed serious tears on the surface of AISI 321 stainless steel, showing typical adhesive wear characteristics after dry friction. In contrast, there existed only shallow furrows as well as mild tears on the surface of Fe–Mn–Si–Cr–Ni–C alloy resulting from the occurrence of the stress-induced $\gamma \rightarrow \varepsilon$ martensitic transformation.

In dry friction, Fe–14Mn–5.5Si–12Cr–5Ni–0.10C shape memory alloy also showed better wear resistance than that AISI 321 stainless steel did, which was different from Lin's study on Fe–17Mn–5Si–10Cr–4Ni alloy. The reason could be attributed to the increase in yield strength of austenite due to solution strengthening of carbon.

The study by Söderberg et al. [17] showed that Fe–Mn–Si–Cr–Ni shape memory alloy with 9–12% Cr did not show passivation in NaCl solution. In this article, the Cr content of the tested Fe–Mn–Si–Cr–Ni–C alloy was 11.54%. This may be the reason that the corrosion rate of the tested alloy was higher in NaCl solution than that of AISI 321 stainless steel with 18% Cr. However, in alkaline environment, the increase in Cr content decreased the corrosion resistance [18]. Therefore, in NaOH solution, the corrosion rate of the tested alloy was lower than that of AISI 321 stainless steel.

Conclusions

Fe–14Mn–5.5Si–12Cr–5Ni–0.10C shape memory alloy showed better wear resistance than that of AISI 321 stainless steel both in dry and oily friction conditions. The occurrence of the stress-induced $\gamma \rightarrow \varepsilon$ martensitic phase transformation in Fe–14Mn–5.5Si–12Cr–5Ni–0.10C alloy accounted for its better wear resistance. In oily friction, the stress-induced $\gamma \rightarrow \varepsilon$ martensitic transformation occurred easier than in dry friction due to the lubricant cooling, thus, it showed better wear resistance than in dry friction. The addition of carbon strengthened austenitic matrix in Fe–14Mn–5.5Si–12Cr–5Ni–0.10C alloy and thus its wear resistance in dry friction was also better than that of AISI 321 stainless steel. The corrosion rate of Fe–14Mn–5.5Si–12Cr–5Ni–0.10C alloy was remarkably lower in NaOH solution and higher in NaCl solution than that of AISI 321 stainless steel.

Acknowledgement The study was supported by the Program for New Century Excellent Talents in University (No. NCET-06-0793).

References

1. Michal GM, Ernst F, Kahn H, Cao Y, Oba F, Agarwal N, Heuer AH (2006) Acta Mater 54:1597
2. Richter E, Guenzel R, Parasacandola S, Telbizova T, Kruse O, Moeller W (2000) Surf Coat Technol 128–129:21
3. Sun Y, Bell T (1998) Wear 218:34
4. Lei MK, Zhu XM (2005) Surf Coat Technol 193:22
5. Viswanathan A, Sastikumar D, Rajarajan P, Kumar H, Nath AK (2007) Opt Laser Technol 39:1504
6. Wei R (1996) Surf Coat Technol 83:218
7. Flis J, Mankowski J, Rolinski E (1989) Surf Eng 5:151
8. Rolinski E (1987) Surf Eng 3:35
9. Yamauchi N, Okamoto A, Tukahara H, Demizu K, Ueda N, Sone T, Hirose Y (2003) Surf Coat Technol 174–175:465
10. Otsuka H, Tanasashi H et al (1990) Mater Sci Forum 5:451
11. Zhu XM, Zhang YS (1997) J Mater Sci Lett 16:1516
12. Sato A, Chishima E, Soma K, Mori T (1982) Acta Metall 30:1177
13. Sato A, Chishima E, Yamaji Y, Mori T (1984) Acta Metall 32:539

14. Otsuka H, Yamada H, Maruyama T, Tanasashi H et al (1990) ISIJ Int 30:674
15. Wen YH, Yan M, Li N (2004) Scr Mater 50:441
16. Lin CX, Wang GX, Wu YD, Wang JG, Zhang JJ (2006) Mater Sci Eng A 438–440:804
17. Söderberg O, Liu XW, Yakovenko PG, Ullakko K, Lindroos VK (1999) Mater Sci Eng A 273–275:543
18. Huang X, Wan JF, Chen SP, Hsu TY (2002) J Shanghai Jiaotong Univ 36:21